Applied Catalysis B: Environmental 140–141 (2013) 406–411

Contents lists available at SciVerse ScienceDirect

Applied Catalysis B: Environmental

journal homepage: www.elsevier.com/locate/apcatb

Influence of co-existing alcohol on charge transfer of H_2 evolution under visible light with dye-sensitized nanocrystalline TiO_2 ☆

Masato M. Maitani [a,*], Conghong Zhan [a,b], Dai Mochizuki [a], Eiichi Suzuki [a], Yuji Wada [a,*]

[a] Department of Applied Chemistry, Tokyo Institute of Technology, 2-12-1 Ookayama, Meguro, Tokyo 152-8552, Japan
[b] College of Chemistry, JiLin University, Changchun 130012, PR China

ARTICLE INFO

Article history:
Received 23 January 2013
Received in revised form 9 April 2013
Accepted 15 April 2013
Available online 25 April 2013

Keywords:
Dye-sensitization
TiO_2
Water splitting
Photocatalysts
Electron transport

ABSTRACT

The dye-sensitized nanocrystalline TiO_2 colloidal suspension in aqueous systems has been applied for H_2 evolution in the photocatalytic water splitting under visible irradiation. We have reported that the conversion efficiency is strongly influenced by the combination of dye-sensitizers and co-existing species in the suspension system. We herein analyze the fluorescence quenching of the dye-sensitized TiO_2 nanoparticles in the suspensions and photoelectrochemical properties of dye-sensitized nanoporous TiO_2 films. The combination of dye-sensitizers and co-existing species dominates the charge recombination resulting in significant differences in the efficiencies of the proton reduction into H_2.

© 2013 The Authors. Published by Elsevier B.V. All rights reserved.

1. Introduction

Artificial photosynthetic systems for direct conversion of water to obtain an energy source, hydrogen, under sunlight are of great interest and importance for renewable energy used in the future. Wide-band gap nano-sized semiconductor materials such as metal oxide, nitride, and sulfide derivatives have been widely studied to harvest light to generate electrons with high energy capable of reduction of protons to H_2 and holes are consumed in oxidation of sacrificial electron donors, redox shuttles, or water [1–3]. The advantages of these oxide semiconductors are robustness, abundance of materials, ease of preparation, and non-toxicity. The absorption of band gap transition typically ranges in the ultraviolet region with these semiconductors, while most photon flux from sunlight ranges widely in visible and infrared regions. Therefore harvesting photons in visible and infrared region is one of the most important issues with these semiconductors for photo catalyst development.

As summarized elsewhere [1–4], three types of strategy have been proposed to achieve higher photon collection efficiency under sunlight, *i.e.* (1) introduction of inter-band states by metal or non-metal doping, (2) adjustment of band structures by solid solution or single-phase heterometallic oxide, and (3) dye-sensitization by chromophore molecules. Among those, the dye-sensitization of the semiconductors by organic or inorganic dyes has elegantly enabled the high solar energy conversion efficiency of ~12% owing to the almost 100% internal quantum efficiency in the photon-to-electron conversion process in the visible region, 400–700 nm, for a photovoltaic device known as the dye-sensitized solar cells [6,7]. Nevertheless, the dye-sensitization system for photocatalytic water splitting still remains relatively less efficiency than other systems. One of general concerns of dye-sensitization system is the lack of stability of dye-sensitizers under photocatalytic reaction in water. Recent reports, however, revealed that the durability problem of dye-sensitizers is possibly overcome by using robust dye-sensitization system revealing continuous H_2 evolution for more than hundreds of hours [7,8]. Furthermore the complete water splitting, both H_2 and O_2 evolution, has been also achieved with dye-sensitization system by applying the other catalysts, such as WO_3, IrO_2, or Co [9–11]. One of the great advantages of the dye-sensitization system is ultrafast charge separation producing an electron and a hole at the dye–semiconductor interface [6]. The spatial charge separation achieved by the electron injection from dye-sensitizers into semiconductors dramatically suppresses the charge recombination of electrons and holes. The charge separation process is thus efficient enough to reach 100% quantum yield in the dye-sensitization system [4,6]. The electron injection occurs from the lowest unoccupied molecular orbital (LUMO) locating at

☆ This is an open-access article distributed under the terms of the Creative Commons Attribution License, which permits unrestricted use, distribution and reproduction in any medium, provided the original author and source are credited.

* Corresponding authors. Tel.: +81 5734 2879; fax: +81 5734 2879.
E-mail addresses: mmaitani@apc.titech.ac.jp (M.M. Maitani), yuji-w@apc.titech.ac.jp (Y. Wada).

0926-3373/$ – see front matter © 2013 The Authors. Published by Elsevier B.V. All rights reserved.
http://dx.doi.org/10.1016/j.apcatb.2013.04.044

more negative chemical potential than that of the conduction band (CB) of semiconductors [6,12]. Therefore, the injection efficiency is closely related to the potential gap between CB and LUMO [13–16], while the electron injection strongly affecting on the efficiency of the photoelectric conversion also depends on other factors, *e.g.* aggregation of dye molecules on the surface, the co-existing species and its adsorption on the surface of semiconductors, and solvent effects [17–21]. It is, however, generally considered that the dye-sensitization system has not been completely understood especially in case co-existing species are involved in the system [22–25]. The study to comprehend the complex system including co-existing species, *e.g.* contaminants, acid, base, and electrolytes, in dye-sensitized photocatalytic water splitting process is highly desirable for the realistic application for large water supply in our society; such as waste water from residential or industrial area and natural water in sea or lakes [26,27]. We recently reported that the electron injection process of dye-sensitization system strongly depends on the co-existing species, MeOH and TEOA, as the sacrificial electron donors in surrounding solution for the photocatalytic H_2 evolution [28,29]. It was, however, found that the capability of H_2 evolution cannot be attributed to only electron injection efficiency but also other electron transfer processes at the dye/TiO_2 interface.

We herein focus on the differences of effects of co-existing species on the photocatalytic H_2 evolution with N719/TiO_2 and porphyrin derivatives/TiO_2 especially the photo-induced electron transfer processes. A series of photochemical and photoelectrochemical analyses are carried out to elucidate the effect of the co-existing electron donors, MeOH and TEOA, in the surrounding medium. We therefore discuss the combinational effects between the dye-sensitizers and donor species on the electronic structures and dye adsorption properties at dye/TiO_2 interfaces determining the electron transfer processes in photocatalytic H_2 evolution.

2. Experimental

2.1. Materials

The commercially available TiO_2 particles (P25, Nippon Aerosil), dye-sensitizers, (*n*-$Bu_4N)_2$-*cis*-Ru(dcbpy)$_2$(SCN)$_2$ (N719, Solaronix, Switzerland), tetrakis(4-carboxyphenyl)porphyrin and tetrakis(4-sulfonatophenyl)porphyrin (TCPP and TPPS, respectively, Tokyo Kasei) were used as purchased without any further purification.

2.2. Sample preparation

For hydrogen evolution, loading of Pt on oxide semiconductors was employed by a conventional photochemical deposition to obtain 1 wt% Pt-loaded TiO_2 nanoparticles as described elsewhere [28,29]. The dye-sensitized Pt-loaded TiO_2 nanoparticles were obtained by dispersing Pt-loaded TiO_2 nanoparticles into 0.1 mM of dye-sensitizers in methanolic solution, kept for 48 h under dark, filtrated, washed with deionized water, and then dried at 80 °C. The adsorption isotherm of the dye-sensitizers on TiO_2 revealed monolayer chemisorptions by carboxylic and sulfonic acid moiety of the dyes (S1). For photoelectrochemical analysis, the dye-sensitized nanoporous TiO_2 films were prepared by the conventional doctor blade technique by using commercially available TiO_2 paste (Ti-nanoxide D, Solaronix) on cleaned F:SnO_2 transparent conductive glass (TCO) and sintered at 450 °C for 30 min in atmosphere. To avoid the leaks current from TCO, the TCO substrate was covered by compact TiO_2 layer by immersion of TCO in $TiCl_4$ aqueous solution for 45 min at 70 °C [4–6]. When the temperature was dropped to 80 °C after sintering, these films were immersed into a 0.1 mM solution of dye-sensitizers in methanolic solution, kept under dark for 12 h, washed by ethanol, and then dried under N_2 flow.

2.3. H_2 evolution

The H_2 evolution was performed in an outer irradiative photoreactor under a Xe lamp (LC8, HAMAMATSU) irradiation through a cut-off filter (λ < 390 nm cut, UV-39, TOSHIBA). The dye-sensitized Pt-loaded TiO_2 nanoparticles were dispersed in an aqueous solution (1 g/L) containing sacrificial electron donors, MeOH and TEOA. Prior to the irradiation, an ultrasonication for 5 min and consecutively argon bubbling for 15 min were applied to the reaction mixture. The evolved H_2 was analyzed by taking the sample gas from the photoreactor with a gas-tight syringe every 5 min and evaluated by a gas chromatography (molecular sieve 5A column with Ar carrier gas, GC-8A, Simadzu). As a controlled experiment with D_2O solution, all evolved hydrogen was D_2 ensuring that the hydrogen source is the protons in the water not from other compounds, such as donor species or dye-sensitizers. Another controlled experiment without dye-sensitizer also ensured that the residual UV light is negligible for H_2 evolution.

2.4. Fluorescence quenching analysis

The fluorescence spectra of each dye-sensitizer, TCPP and TPPS in the aqueous sacrificial donor solutions with varying the density of TiO_2 colloids were measured to study the electron injection processes. A TiO_2 stock suspension in water (~4 g/L) was prepared by ultrasonication for more than 30 min giving monodispersive colloidal suspension confirmed by a dynamic light scattering measurement. The fluorescence spectra of dye-sensitizer in aqueous solution were collected in a 1 cm-quartz-cell under photo-excitation (λ = 410 nm (TCPP) and 415 nm (TPPS), F7000, Hitachi). The specific amount of the TiO_2 stock suspension was successively added dropwisely into the dye-sensitizer solution and then the fluorescence spectra were measured after waiting for 15 min to reach equilibrium. The concentrations of either TEOA in MeOH (6.2 M) or MeOH in TEOA (0.3 M) were also varied to determine the effect of co-existing electron donor species on the fluorescence of dye-sensitizers. All experiments were carried out after 15 min Ar purge and at room temperature. The intensity of fluorescence was determined at the peak top locating at around ~650 nm.

2.5. Electrochemical analysis

The photoelectrochemical analysis was employed with dye-sensitized TiO_2 nanoporous films as a working electrode in a three component electrochemical cell with the aqueous electron donor solution containing 0.1 M of KCl as supporting electrolyte, Pt counter electrode, and a reference electrode, Ag/AgCl, configured with an electrochemical potentiostat (SP-200, Bio-Logic). Ar babbling was applied for 15 min prior to each measurement. A Xe lamp (MAX-302, Asahi bunko) with a cut filter (<410 nm cut, UV-41, TOSHIBA), was used for a visible light source. The residual UV light was confirmed to be negligible by a controlled experiment without dye-sensitizer on TiO_2 film.

3. Results and discussion

3.1. H_2 evolution

As we have reported recently, all three sensitizers, N719, TCPP, and TPPS, revealed continuous H_2 evolution in TEOA solution up to 3 h under visible irradiation [29] (S2). TCPP and TPPS, however, revealed no H_2 evolution in MeOH solution, while N719 resulted in

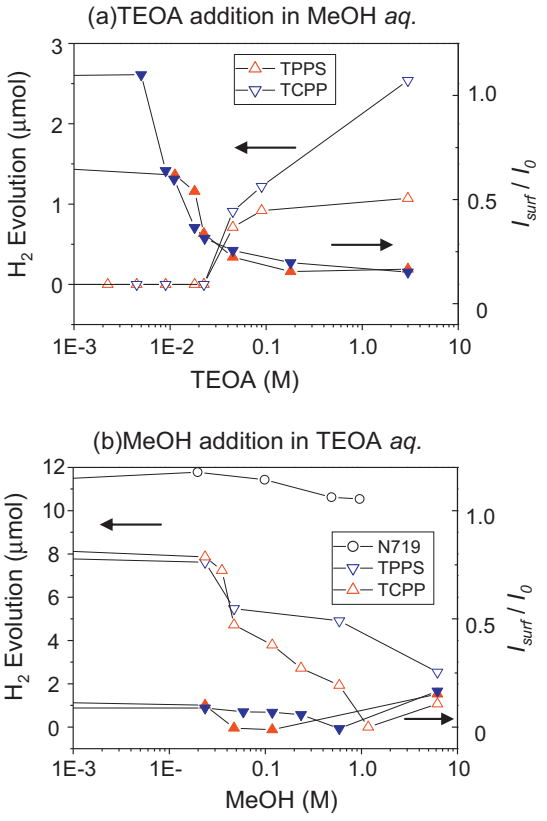

Fig. 1. H_2 evolution (open) and fluorescence quenching efficiency of dye-sensitizers (filled), TCPP (red), TPPS (blue), and N719 (black) on TiO_2 nanoparticles in donor solutions of (a) MeOH and (b) TEOA aqueous solution with addition of either (a) TEOA or (b) MeOH, respectively, under visible light (>390 nm: Xe lamp). (For interpretation of the references to color in this figure legend, the reader is referred to the web version of this article.)

comparable reaction even in MeOH solution. The produced H_2 gas in the photoreactor after 3 h reaction was quantitatively plotted as a function of the concentration of electron donors, either TEOA in MeOH (6.2 M) or MeOH in TEOA (0.3 M), in Fig. 1. Although both TEOA and MeOH are typical electron donors used in photocatalysts systems (E_{ox} = 0.2–0.7 V (MeOH) [30,31] and E_{ox} = 0.82 V (TEOA) [32] *vs.* NHE, respectively), and also HOMO levels of TCPP (0.96 V *vs.* NHE), TPPS (0.98 V *vs.* NHE), and N719 (0.85 V *vs.* NHE) are located closely [33–35], the resulted H_2 evolution shows clear difference depending on the combination of dye-sensitizers and co-existing electron donor species in the aqueous solution.

3.2. Fluorescence quenching analysis

To study the efficiencies of electron injection at dye-sensitizers/TiO_2 interface in each system, we employed a fluorescence quenching measurement of dye-sensitizers by addition of the accepter, TiO_2 nanoparticles, for the photo-excited electron transfer known as Stern–Volmer relation [15,36–39]. Because of the lack of fluorescence intensity with N719, we applied this analysis only to the systems with porphyrin/TiO_2 colloidal suspension. Since each dye-sensitizer interacts with TiO_2 nanoparticles with certain association constants, K_{app} [15,28], we apply the reciprocal Stern–Volmer relation under a consideration of an association constant, as indicated by Eq. (1), where I_{surf} represents the fluorescence intensity of dye-sensitizer in case all of dye molecules in the system is adsorbed on the quencher, TiO_2, with an infinity amount of quencher with an association constant, K_{app} [28,39]. We multiply both sides of Eq. (1) by I_0 to deliver the I_{surf}/I_0

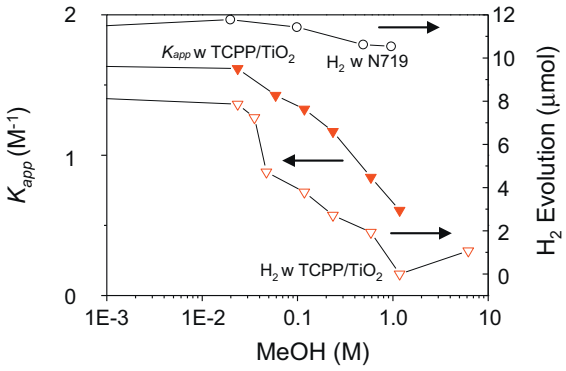

Fig. 2. The association constants (filled red triangle) calculated from the reciprocal Stern–Volmer plots and H_2 evolution of TCPP/TiO_2 (open red triangle) and N719/TiO_2 (open black circle) as a function of the concentrations of co-existing electron donor, MeOH, in TEOA (0.3 M) aqueous solutions. (For interpretation of the references to color in this figure legend, the reader is referred to the web version of this article.)

from the intercept as indicated in Eq. (2). To elucidate the detailed effect of MeOH and TEOA on electron injection at dye/TiO_2 interfaces reflected as the fluorescence quenching and the capability of photocatalytic H_2 evolution, I_{surf}/I_0 calculated from the reciprocal Stern–Volmer plots are overlaid on the H_2 evolution as a function of the concentrations of aqueous solutions of either TEOA in MeOH (6.2 M) or MeOH in TEOA (0.3 M) in Fig. 1 [29].

$$\frac{1}{I_0 - I} = \frac{1}{I_0 - I_{surf}} + \frac{1}{K_{app}(I_0 - I_{surf})[Q]} \quad (1)$$

$$\frac{I_0}{I_0 - I} = \frac{I_0}{I_0 - I_{surf}} + \frac{I_0}{K_{app}(I_0 - I_{surf})[Q]} \quad (2)$$

As we reported recently, lower value of I_{surf}/I_0 results in higher efficiency of H_2 evolution by addition of TEOA in MeOH with porphyrin dye/TiO_2 systems. Therefore we concluded that the co-existing TEOA dramatically improves the electron injection efficiency at dye/TiO_2 interface [29]. On contrary, no correlation was observed between the efficiency of the electron injection and the H_2 evolution by addition of MeOH in TEOA (Fig. 1b). In these series of data, the porphyrin dye/TiO_2 systems in TEOA (0.3 M) solution achieved almost complete electron injection at dye/TiO_2 interface as indicated with sufficiently low value of I_{surf}/I_0. This is because of the same effect of TEOA addition in MeOH system revealed above (Fig. 1a); *i.e.* high concentration of TEOA provides efficient electron injection ability [29]. H_2 evolution, however, significantly decreased by addition of MeOH in TEOA solution, although high efficiency of the electron injection remains stationary in the whole range of MeOH concentration in TEOA solution.

To elucidate the effect of MeOH addition in TEOA, the association constants, K_{app}, of dye-sensitizers with TiO_2 nanoparticles were also calculated from the reciprocal Stern–Volmer analysis and overlaid on the H_2 evolution as well (Fig. 2). This plot revealed that H_2 evolution and the association constants similarly decrease above the MeOH concentration of around $\sim 10^{-2}$ M in TEOA solution. In case of N719/TiO_2, the effect of MeOH concentration on dye adsorption was examined by the optical absorption of dissociated dye into donor solution (S3), since the Stern–Volmer analysis cannot be applied to N719. On contrary to porphyrin dye/TiO_2 system, the dye adsorption property of N719/TiO_2 revealed stationary through the concentration of MeOH in TEOA within the experimental conditions. Since TCPP and TPPS revealed similar trends, we focus on the difference between Ru dye and porphyrin dye represented by N719 and TCPP, respectively.

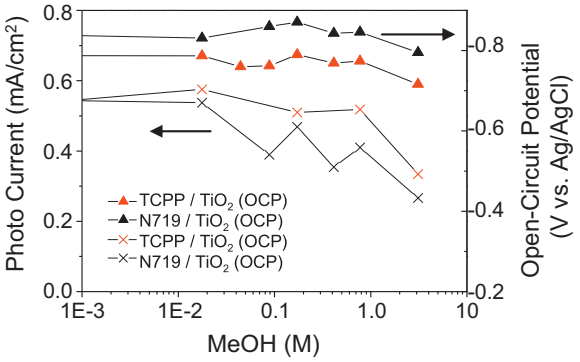

Fig. 3. Photo-current (at 0.1 V *vs.* Ag/AgCl) and open-circuit potential (*vs.* Ag/AgCl) of TCPP (red) and N719 (black) on TiO_2 under visible light irradiation as a function of MeOH concentration in TEOA (0.3 M) aqueous solution. (For interpretation of the references to color in this figure legend, the reader is referred to the web version of this article.)

3.3. Electrochemical analysis

Photoelectrochemical analyses were also carried out with dye/TiO_2 porous films in aqueous TEOA (0.3 M) solution. The photocurrent and dark current are correlated with a manipulated shutter of incident light at the potential of 0.1 V (*vs.* reference electrode (RE): Ag/AgCl) on the working electrode, dye/TiO_2 nanoporous films. A clear photo response as the anodic current was observed due to the collection of electron injected from dye-sensitizers under irradiation on the conducting glass electrode as the working electrode (S4). The applied potential was chosen to observe only the photo current generated by the dye-sensitization of TiO_2 under irradiation, since negligible dark current was observed at the applied potential (S4). The photocurrent at 0.1 V *vs.* RE and open-circuit potential under visible irradiation are plotted as a function of MeOH concentration in aqueous TEOA (0.3 M) solution in order to examine the effect of MeOH addition on the photon-to-current conversion efficiency and quasi-Fermi level (Fig. 3), respectively. Fig. 3 indicates that both photocurrent and open-circuit potential exhibits stationary within the whole range of MeOH concentration, but a slight decline was observed with the MeOH concentration above $\sim 10^{-2}$ M in TEOA solution. This trend is similar to that of I_{surf}/I_0 in Fig. 1b, *i.e.* slight decline of charge transfer efficiency was observed by addition of MeOH with a concentration above $\sim 10^{-2}$ M in TEOA solution. Therefore, the trend of photocurrent and open-circuit potential under irradiation reflects the electron injection efficiency at dye/TiO_2 interface. This can be because of MeOH effect suppressing the electron injection as previously reported [29]. Nevertheless, a large difference between two systems, N719/TiO_2 and TCPP/TiO_2, was clearly observed as the open-circuit potential difference of 50–100 mV in between. This open-circuit potential difference could be attributed to the pH difference in the solution containing N719 and TCPP as discussed in detail below.

We examined the onset potential of cathodic current of dye/TiO_2 nanoporous films in the cyclic voltammogram in the electron donor solutions under dark, which qualitatively represents the conduction band edge of TiO_2 semiconductor (Fig. 4). The onset potential of the TCPP/TiO_2 film positively shifts by addition of MeOH. The inset plotting the onset potential as the average of potentials on cathodic and anodic sweep revealing cathodic current of 2 μA qualitatively indicates a shift of onset potential with a threshold concentration of $\sim 10^{-2}$ M, which reveals quite similar to the trend of decline with H_2 evolution (Fig. 1b). On contrary, N719/TiO_2 film exhibits no decline both with the onset potential and H_2 evolution by addition of MeOH, and remains stationary (Figs. 1b and 4a).

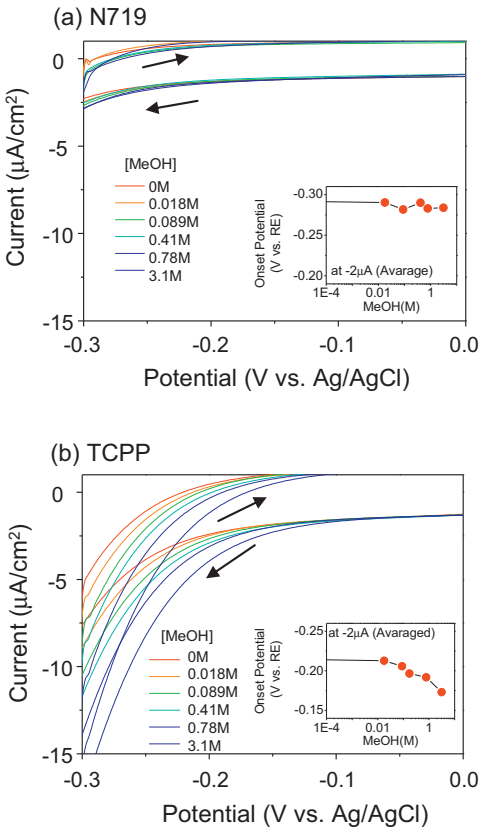

Fig. 4. Cyclic-voltamograms of (a) N719 and (b) TCPP dye-sensitized TiO_2 porous films in TEOA solution (0.3 M) by varying MeOH concentration. Arrows indicate the direction of voltage swipes. The insets indicate the reduction current of dye-sensitized TiO_2 film at −0.25 V (*vs.* Ag/AgCl) qualitatively representing the change of onset potential of TiO_2.

As observed in open-circuit potential under irradiation (Fig. 3), N719/TiO_2 and TCPP/TiO_2 clearly revealed the difference of onset potential of ~150 mV, which exhibits even larger difference than that of open-circuit potential; *i.e.* 50–100 mV (Fig. 3).

3.4. Effect of MeOH on electron transport and H_2 evolution

Here we discuss the difference of MeOH effect between N719/TiO_2 and TCPP/TiO_2 systems in terms of (1) electronic structure of conduction band and (2) dye adsorption on TiO_2. According to the Nernstian behavior of the conduction band potential shift of TiO_2 with a 59 meV/pH unit [40,41], the pH range by addition of MeOH, pH 7.5–8.5 (S5), results in the positive shift of conduction band of 50–100 mV. The positive shifts of open-circuit potential (Fig. 3) and onset potential (Fig. 4b) by the addition of MeOH are thus attributed to the pH effect on conduction band due to the acidic MeOH. Although the pH shifts the conduction band of TiO_2, the potential of electron reducing the proton cannot be changed according to the Nernstian potential shift of the reduction potential of protons in the aqueous mediator. Therefore the rate constant of H_2 evolution by photoelectrochemical proton reduction cannot be affected by the conduction band shift by pH change. Consequently, the large difference of onset potential or open circuit potentials between N719/TiO_2 and TCPP/TiO_2 systems are not clearly attributed to the pH effects. And furthermore the large onset potential shift observed in cyclic voltammogram of only TCPP/TiO_2 by addition of MeOH (Fig. 4) are not correlated to the pH change by addition of MeOH; *i.e.* N719 system is more basic with a pH unit of 1 than TCPP system due to its basicity of N719 dye, while pH difference of 1 (S5) is not equivalent to the onset

shift of ~150 mV based on Nernstian behavior of TiO_2 (59 mV/pH unit). One possible explanation of the difference could be the nature of the dye/TiO_2 interfaces with acidic TCPP and basic N719, since N719 with basic tetrabutylammonium moiety was proposed to negatively shift the conduction band potential of TiO_2 to gain the open-circuit voltage of dye-sensitized solar cells [16]. According to these results, the positive potential shift of the conduction band of TiO_2 caused by MeOH addition would significantly lower the potential of injected electron in TiO_2, and thereby degrades the capability of reduction of protons in the solution for photocatalytic H_2 evolution. Therefore the deactivation path of injected electron, charge recombination, becomes relatively dominant. N719/TiO_2, however, possesses 100–150 mV more negative potential of injected electron than TCPP/TiO_2 (Figs. 3 and 4b). This potential difference thus causes the clear difference in reaction path of injected electron between N719/TiO_2 and TCPP/TiO_2 systems with MeOH addition in aqueous TEOA solution and therefore results in the efficiency of H_2 evolution.

As another factor, the surface adsorption of dye on TiO_2 surface is taken into the consideration to understand the effects of MeOH addition. Since the fluorescence quenching analysis (Fig. 1) and photocurrent in photoelectrochemical analysis (Fig. 3) confirmed that both N719/TiO_2 and TCPP/TiO_2 have efficient electron injection at dye/TiO_2 interface within the given range of MeOH addition. Therefore the limiting factor of H_2 evolution is attributed to any of successive processes following to the electron injection. The charge recombination thus would be one of the controlling factors of H_2 evolution in TEOA solution. We attribute the effects of the MeOH addition in TEOA on H_2 evolution to the surface adsorption characteristics of dye on TiO_2 [6,21]. MeOH addition decreases the association constant of porphyrin with TiO_2, especially with the MeOH concentration above ~10^{-2}M (Fig. 3). Although the association constant of N719 cannot be measured in our experimental condition in fluorescence measurement, the adsorption amount of dye on TiO_2 was examined by the control experiment of dye desorption in aqueous TEOA/MeOH solution as a function of MeOH concentration (S3). The adsorption of N719 is inert for MeOH addition. Furthermore, the clear correlation observed with association constant and H_2 evolution strongly supports that the limiting factor is related to the dye adsorption characteristics. Therefore one possible mechanism of increase in recombination can be attributed to loosening the porphyrin dye adsorption characteristics on TiO_2 surfaces probably exposing surface recombination centers, for example, surface defects or oxygen vacancies. The adsorption or desorption of dyes would strongly influence the electron transfer processes resulting in difference of charge recombination kinetics as reported [6,16–21]. According to the results of dye adsorption, TCPP/TiO_2 possibly more affected by MeOH thus likely exposing more surface recombination centers on TiO_2, although the coverage of N719 and TCPP revealed stationary within the experimental conditions (S3). Furthermore, the strength of adsorption of dye-sensitizers also affects the orientation of organic dyes, such as porphyrin, while spherical dye-sensitizers, such as Ru complex, are inert for the orientation of dyes [42,43]. These differences of dye adsorption nature of porphyrin and Ru complex dye-sensitizers may result in the different recombination kinetics in case of MeOH addition.

Consequently, the dye adsorption may affect (1) the electronic structure of the TiO_2 and (2) dye-adsorption amount, which could lower quasi-Fermi level and enhance the recombination, respectively, and therefore suppress the proton reduction evolving H_2. Since N719 has been utilized to the dye-sensitized solar cells for its ability of slow charge recombination, it is understandable that the adsorption nature of N719 may provide more inert dye/TiO_2 interface to the environment in terms of the charge recombination as observed in Figs. 3 and 4 [44].

4. Conclusion

To summarize, we performed the analyses of the photochemical properties based on the reciprocal Stern–Volmer relation and the photoelectrochemical properties of dye/TiO_2 porous films in order to elucidate the effect of MeOH addition in aqueous TEOA solution revealing significant difference in H_2 evolution between N719/TiO_2 and TCPP/TiO_2. The observed differences are attributed to the electron recombination kinetics following to the sufficient electron injection process in aqueous TEOA solution. The recombination process becomes competitive or even dominant process against the proton reduction process by addition of MeOH, because of either increase of recombination rate or the lack of reduction potential of reactive electron in the TiO_2. This effect is still minor with N719/TiO_2 as compared with TCPP/TiO_2. This difference is possibly attributed to the adsorption nature of dye-sensitizers, N719 and TCPP on TiO_2 nano particles. We are now studying these effects on different nanocrystalline oxide semiconductor systems to reveal a dependence of observed effects on semiconductor material characteristics as a future work.

Appendix A. Supplementary data

Supplementary data associated with this article can be found, in the online version, at http://dx.doi.org/10.1016/j.apcatb.2013.04.044.

References

[1] X. Chen, S. Shen, L. Guo, S.S. Mao, Chemical Reviews 110 (2010) 6503–6570.
[2] A. Fujishima, X. Zhang, D.A. Tryk, Surface Science Reports 63 (2008) 515–582.
[3] M.G. Walter, E.L. Warren, J.R. McKone, S.W. Boettcher, Q. Mi, E.A. Santori, N.W. Lewis, Chemical Reviews 110 (2010) 6446–6473.
[4] A. Hagfeldt, M. Grätzel, Chemical Reviews 95 (1995) 49–68.
[5] B. O'Regan, M. Grätzel, Nature 353 (1991) 737–740.
[6] A. Hagfeldt, G. Boschloo, L. Sun, L. Kloo, H. Pettersson, Chemical Reviews 110 (2010) 6595–6663.
[7] R. Abe, K. Hara, K. Sayama, K. Domen, H. Arakawa, Journal of Photochemistry and Photobiology A 137 (2000) 63–69.
[8] Z. Jin, X. Zhang, G. Lu, S. Li, Journal of Molecular Catalysis A 259 (2006) 275–280.
[9] W.J. Youngblood, S.-H.A. Lee, Y. Kobayashi, E.A. Hernandez-Pagan, P.G. Hoertz, T.A. Moore, A.L. Moore, D. Gust, T.E. Mallouk, Journal of the American Chemical Society 131 (2009) 926–927.
[10] R. Abe, K. Shinmei, K. Hara, B. Ohtani, Chemical Communications (2009) 3577–3579.
[11] T.T. Lea, M.S. Akhtara, D.M. Park, J.C. Lee, O-B. Yang, Applied Catalysis B 111–112 (2012) 397–401.
[12] B.C. O'Regan, J.R. Durrant, Accounts of Chemical Research 42 (2009) 1799–1808.
[13] K. Hara, T. Sato, R. Katoh, A. Furube, Y. Ohga, A. Shinpo, S. Suga, K. Sayama, H. Sugihara, H. Arakawa, Journal of Physical Chemistry B 107 (2003) 597–606.
[14] Y. Tachibana, M.K. Nazeeruddin, M. Grätzel, D.R. Klug, J.R. Durrant, Chemical Physics 285 (2002) 127–132.
[15] K. Kalyanasundaram, N. Vlachopoulos, V. Krishnan, A. Monnier, M. Grätzel, Journal of Physical Chemistry 91 (1987) 2342–2347.
[16] J.B. Asbury, N.A. Anderson, E. Hao, X. Ai, T. Lian, Journal of Physical Chemistry B 107 (2003) 7376–7386.
[17] J.-H. Yum, S.-R. Jang, R. Humphry-Baker, M. Grätzel, J.-J. Cid, T. Torres, M.K. Nazeeruddin, Langmuir 24 (2008) 5636–5640.
[18] A. Kay, M. Grätzel, Journal of Physical Chemistry 97 (1993) 6272–6277.
[19] N.R. Neale, N. Kopidakis, J. van de Lagemaat, M. Grätzel, A.J. Frank, Journal of Physical Chemistry B 109 (2005) 23183–23189.
[20] D.F. Watson, G.J. Meyer, Coordination Chemistry Reviews 248 (2004) 1391–1406.
[21] J.A. Pollard, D.S. Zhang, J.A. Downing, F.J. Knorr, J.L. McHale, Journal of Physical Chemistry A 109 (2005) 11443–11452.
[22] D.N. Furlong, D. Wells, W.H.F. Sasse, Journal of Physical Chemistry 90 (1986) 1107–1115.
[23] E. Bae, W. Choi, Journal of Physical Chemistry B 110 (2006) 14792–14799.
[24] S.K. Choi, H.S. Yang, J.H. Kim, H. Park, Applied Catalysis B 121–122 (2012) 206–213.
[25] K. Kalyanasundaram, J. Kiwi, M. Gräzel, Helvetica Chimica Acta 61 (1978) 2720–2730.
[26] M.D. Hernández-Alonso, F. Fresno, S. Suárez, J.M. Coronado, Energy & Environmental Science 2 (2009) 1231–1257.
[27] L. Zhang, W. Wang, S. Sun, Y. Sun, E. Gao, J. Xu, Applied Catalysis B 132–133 (2013) 315–320.

[28] C. Zhan, M.M. Maitani, D. Mochizuki, E. Suzuki, Y. Wada, Chemistry Letters 41 (4) (2012) 423–424.
[29] M.M. Maitani, C. Zhan, C.-C. Huang, C.-C. Hu, D. Mochizuki, E. Suzuki, Y. Wada, Bulletin of the Chemical Society of Japan 85 (2012) 1268–1276.
[30] T. Iwasita, Electrochimica Acta 47 (2002) 3663–3674.
[31] S. Wasmus, A. Küver, Journal of Electroanalytical Chemistry 461 (1999) 14–31.
[32] M. Kirch, J.-M. Lehn, J.-P. Sauvage, Helvetica Chimica Acta 62 (1979) 1345–1384.
[33] K. Kalyanasundaram, M. Neumann-Spallart, Journal of Physical Chemistry 86 (1982) 5163–5169.
[34] A. Kathiravan, R. Renganathan, Journal of Colloid and Interface Science 331 (2009) 401–407.
[35] M.K. Nazeeruddin, A. Kay, I. Rodicio, R. Humphry-Baker, E. Miiller, P. Liska, N. Vlachopoulos, M. Grätzel, Journal of the American Chemical Society 115 (1993) 6382–6390.
[36] S. Hirayama, Journal of the Chemical Society, Faraday Transactions 1 78 (1982) 2411–2421.
[37] J.M. Masnovi, E.D. Seddon, J.K. Kochi, Canadian Journal of Chemistry 62 (1984) 2552–2559.
[38] P.V. Kamat, W.E. Ford, Chemical and Physical Letters 135 (1987) 421–426.
[39] P.V. Kamat, J.-P. Chauvet, R.W. Fessenden, Journal of Physical Chemistry 90 (1986) 1389–1394.
[40] T. Watanabe, A. Fujishima, K.-I. Honda, Chemistry Letters (1974) 897–900.
[41] J.M. Bolts, M.S. Wrighton, Journal of Physical Chemistry 80 (1976) 2641–2645.
[42] M. Hahlin, E.M.J. Johansson, S. Plogmaker, M. Odelius, D.P. Hagberg, L. Sun, H. Siegbahn, H. Rensmo, Physical Chemistry Chemical Physics 12 (2011) 1507–1517.
[43] A. Fillinger, B.A. Parkinson, Electrochemical Society Journal 146 (1999) 4559–4564.
[44] B.C. O'Regan, K. Walley, M. Juozapavicius, A. Anderson, F. Matar, T. Ghaddar, S.M. Zakeeruddin, C. Klein, J.R. Durrant, Journal of the American Chemical Society 131 (2009) 3541–3548.